Time-Resolved Resonance Raman and Density Functional Theory Investigation of the Photochemistry of (*S*)-Ketoprofen

Yung Ping Chuang, Jiadan Xue, Yong Du, Mingde Li, Hui-Ying An, and David Lee Phillips*

Department of Chemistry, The University of Hong Kong, Pokfulam Road, Hong Kong, People's Republic of China

Received: April 8, 2009; Revised Manuscript Received: June 3, 2009

Ketoprofen is known to induce photosensitivity due to its specific structure and electronic features, and this limits its use in medical applications. In this Article, the photochemistry of (*S*)-ketoprofen has been investigated by time-resolved resonance Raman spectroscopy to gain additional information so as to better elucidate the possible photochemical reaction mechanism of ketoprofen in different solvents. In nonaqueous solvents like neat acetonitrile and isopropyl alcohol, and 1:1 acetonitrile:water and 1:1 acetonitrile:acidic water aqueous solvents, (*S*)-ketoprofen exhibits benzophenone-like photochemistry to produce a triplet state, which in turn produces a ketyl radical-like species that then undergoes a cross-coupling reaction with either a dimethyl radical (which is generated by hydrogen abstraction of isopropyl alcohol) or a water molecule, respectively, at the *para*-position to form a transient species that has a lifetime up to the microsecond time scale. However, photolysis of (*S*)-ketoprofen in a 1:1 acetonitrile:alkaline water solution and 3:7 acetonitrile:phosphate buffered solution appears to undergo a prompt decarboxylation reaction. Only one species was observed in the nanosecond time-resolved resonance Raman experiments under these conditions, and this species was tentatively assigned to be a triplet protonated biradical carbanion.

Introduction

Ketoprofen (KP) is a benzophenone-derived drug that has useful applications as a nonsteroidal anti-inflammatory drug (NSAID) but can undergo photosensitization reactions that may give rise to unwanted phototoxic effects.[1,2] Therefore, it is important to better understand the photochemistry of KP so that improvements in the design of new related drugs can be made that help minimize the phototoxic effects in this class of drugs. The photochemistry of KP has been extensively studied, and transient absorption experiments[3−6] have been performed to search for the reactive intermediates responsible for its phototoxic effects observed under physiological conditions. These experimental results[3−6] found that the photochemistry of KP has an interesting pH-dependent reaction outcome that appears due to the effects of the propionic acid chain. The acidic form of KP acts much like benzophenone to produce a reactive triplet species efficiently due to a high intersystem crossing (ISC) rate. However, the dissociated form of KP undergoes an efficient decarboxylation reaction instead.

There have been different proposed pathways for the decarboxylation of KP under different solvent systems, and these pathways are summarized in Scheme 1. Montis and co-workers proposed that in a phosphate buffered saline (PBS) solution, the deprotonated ketoprofen (KP^-) undergoes intersystem crossing to a triplet state 1.1 that then undergoes an electron shift to form 1.5a and then decarboxylation to form a benzyllic anion 1.3b. A small portion of the species 1.1 can undergo photoionization to form a radical species 1.6a that then loses CO_2 to produce a radical 1.6b that may then further react to produce dimeric products.[7] This mechanism was also consistent with a product analysis done by Miranda and co-workers using HPLC to separate the products after the photolysis of KP at different concentrations in PBS, and they proposed that the triplet state ketoprofen (^3KP) produces a carbanion in which the carbonyl chromophore abstracts a hydrogen from some hydrogen-donating solvents like methanol to form a ketyl radical 1.5c.[8]

Alternatively, Scaiano and co-workers proposed that the photochemistry of KP in aqueous solution is strongly influenced by its acid−base chemistry. The acid form of KP behaves as a typical benzophenone photoreaction, while in the presence of base the singlet excited state of the carboxylate form KP^- will lead to a carbanion structure 1.3a that has a preferred singlet character and a resonance form of biradical 1.3b with a more stable triplet character.[9,10] This proposed mechanism suggests that the photochemistry of KP depends very much on the ratio between the acid and its conjugate base in the ground state. Furthermore, a blue species that was assigned to be carbanion 1.3a could still be observed for hours under controlled conditions in basic tetrafuran (THF), and 1.4b was formed by deprotonation of the ketyl radical 1.4a under basic reaction conditions. The formation of 1.4b is likely to be triplet-mediated because its growth could be quenched by 1-methylnaphthalene.[11] These observations suggest that the singlet and triplet pathways result in the production of different species that are independent of each other.

Borsarelli and co-workers used time-resolved optoacoustic to study the photochemistry of KP at different pH values and found that the 1.1 species undergoes decarboxylation to produce a carbanion 1.3a and 1.3b that did not appear to depend on pH.[12] This observation supports the mechanism proposed by Scaiano and co-workers[9,10] that a prompt decarboxylation occurs rather than by a pathway via an intramolecular electron-transfer step proposed by Montis and co-workers.[7] The decay of the carbanion 1.3a and 1.3b appears clearly pH-dependent due to their different photochemical pathways, and under acidic conditions at a pH = 6.1, a biradical 1.3c was formed by protonation while a product 3-ethylbenzophenone was formed at pH = 10.9 by a protonation reaction with H_2O. Miranda and

* Corresponding author. Telephone: 852-2859-2160. Fax: 852-2857-1586. E-mail: phillips@hkucc.hku.hk.

10.1021/jp903234m CCC: $40.75
Published on Web 07/02/2009

SCHEME 1: Summary of the Proposed Pathways for the Photochemistry of Ketoprofen in Aqueous Solutions

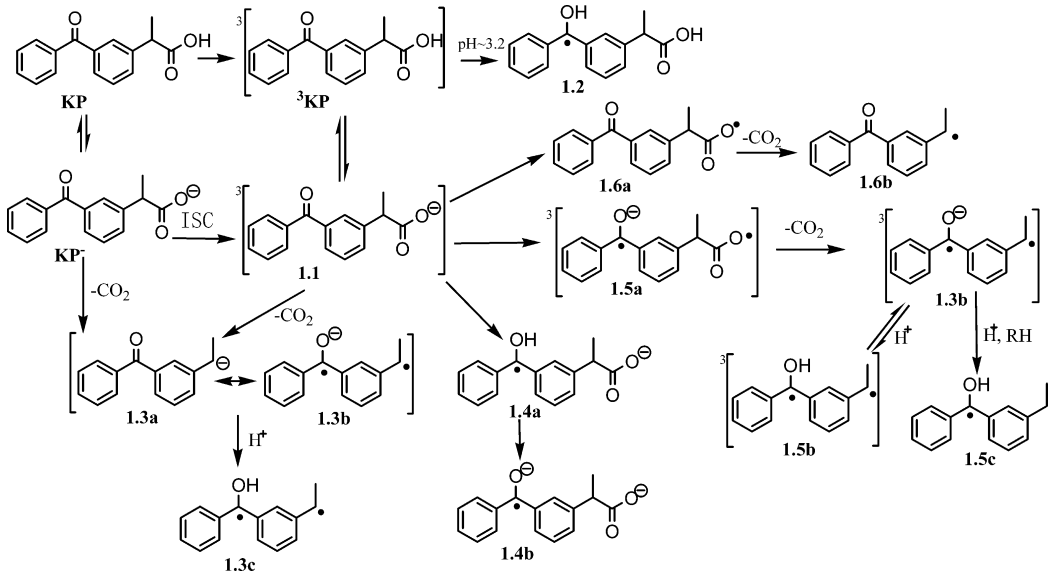

co-workers reported nanosecond laser flash photolysis results that further demonstrated the major pathway occurs via decarboxylation of singlet KP^- to form the carbanions 1.3a and 1.3b at high pH, while the loss of a solvated electron from ^3KP to form 1.6a that subsequently decarboxylates to form 1.6b is a minor pathway.[13]

In contrast, Eriksson and co-workers argued that both the excited singlet states of KP^- and triplet 1.1 undergo decarboxylation readily based on a theoretical study. They found that only a small barrier of 2−3 kcal/mol needed to be overcome for several excited singlet states of KP^-, and a barrier-free pathway was found for the triplet state 1.1 to undergo decarboxylation. They also calculated that the energy of the excited singlet KP^- and triplet 1.1 lies within only a few kcal/mol of each other.[14] This can help explain the high quantum yield observed in the experiments and the short lifetime for the triplet state 1.1. Erikkson and co-workers also suggested that the form of the ground state of KP is crucial for determining the reaction pathways that take place. This was also suggested by Scaiano and co-workers who proposed that only the deprotonated form of KP undergoes the unusual degradation, rather than the neutral form that only undergoes benzophenone-like reactions. At a pH = 3.2, it was proposed that photolysis of KP forms the triplet state ^3KP, the ketyl radical 1.2, and solvated electrons.[9]

Although there have been many studies of the photochemistry of KP, several possible alternative pathways have been proposed, and there is not yet a consensus on the reaction pathways associated with the photochemistry observed under different solvent conditions. It appears further study of the photochemistry of KP is needed to provide additional information about the photochemical pathways. We note that time-resolved vibrational spectroscopy methods like time-resolved resonance Raman (TR^3) spectroscopy that can obtain additional information about the identity, structure, and properties of chemical reaction intermediates have not yet been applied to the photochemistry of KP. We have recently used TR^3 spectroscopy to study the photochemistry of benzophenone (BP) in isopropyl alcohol (IPA) and gained new insight into the identity, structure, and properties of several intermediates associated with the hydrogen abstraction and cross-coupling reactions observed in this system.[15] Because KP is a benzophenone-containing drug, it should be useful to also apply TR^3 spectroscopy to study the photochemistry of KP under different solvent conditions. In this article, nanosecond time-resolved resonance Raman spectroscopy (ns-TR^3) was applied to investigate the dual properties of (*S*)-ketoprofen (SKP) in a variety of organic and aqueous solvents including neat acetonitrile (MeCN), neat isopropyl alcohol (IPA), mixed solvents of 1:1 H_2O:MeCN (by volume), 1:1 $HCl_{(aq)}$:MeCN (by volume) of final pH = 3.2, 1:1 0.1 M $HCl_{(aq)}$:MeCN (by volume), 1:1 0.1 M $HClO_{4(aq)}$:MeCN (by volume), 1:1 PBS:MeCN (by volume), and 1:1 16.4 mM $NaOH_{(aq)}$:MeCN (by volume). These TR^3 results provide valuable vibrational information about the different transient species probed and enable a better understanding of photochemistry of KP in different solvents. The TR^3 experimental results combined with the UV/vis spectra of the KP ground state in different solvents indicate that the reaction pathways of KP are strongly dependent on the form of its ground-state species. KP in 1:1 MeCN:water and 1:1 MeCN:acidic water solutions were found to exhibit benzophenone-like photochemistry to produce a triplet state that reacts with water to produce a ketyl radical-like species. In the presence of a neutral 1:1 MeCN:water solution, a long-lived species 1.2b was observed with a structure similar to the cross-coupled transient species observed in the neat isopropyl alcohol solvent. KP in a 1:1 MeCN:alkaline water solution appears to undergo a very fast decarboxylation reaction, and only one species was observed in the TR^3 experiments under these conditions. This species was found to be sensitive to oxygen, which reveals it has a triplet character. Comparison of the TR^3 spectra and the calculated Raman spectrum for a triplet protonated biradical carbanion (1.3c) generated after decarboxylation shows reasonably good agreement between the spectra. A similar species was also observed after the photolysis of KP in a 3:7 MeCN:PBS, which may imply the degradation of KP under physiological conditions takes place via the decarboxylation process.

Experimental and Computational Methods

Samples of SKP were obtained from Aldrich with 99% purity and used as received. Spectroscopic grade acetonitrile (MeCN), isopropyl alcohol, hydrochloric acid, perchloric acid, sodium hydroxide, potassium dihydrogen phosphate, anhydrous sodium phosphate dibasic, sodium chloride of reagent grade from

Aldrich, 99.9% atom deuterium water from Aldrich, and deionized water were used for preparing sample solutions.

Sample solutions of SKP with concentration ~2 mM in pure MeCN, IPA, and mixed solvents were used in TR^3 experiments. Unless specified, all of the mixed solvent ratios are of volume ratio. There were six sets of sample solutions using 1:1 MeCN:H_2O, 1:1 MeCN:$HCl_{(aq)}$ of final pH = 3, 1:1 MeCN:0.1 M $HCl_{(aq)}$, 1:1 MeCN:0.1 M $HClO_4$, 1:1 MeCN:16.4 mM $NaOH_{(aq)}$, and 3:7 MeCN:PBS as mixed solvents. PBS was prepared by mixing 17 mM KH_2PO_4, 52 mM Na_2HPO_4, and 10 mM NaCl solutions with a final pH = 7.4.

The nanosecond time-resolved resonance Raman (ns-TR^3) experiments were done using an experimental apparatus and methods discussed in detail previously,[16−21] and only a brief description will be given here. The pump laser pulse with a wavelength of 266 nm generated from the fourth harmonic of a Nd:YAG nanosecond pulsed laser and a 319.9 nm probe laser pulse produced from the third anti-Stokes hydrogen Raman shifted laser line from the second harmonic were employed in the TR^3 experiments. The two Nd:YAG lasers were synchronized electronically by a pulse delay generator to control the time delay of pump and probe lasers, and the time delay between the laser pulses was monitored by a fast photodiode and 500 MHz oscilloscope. The time resolution for the TR^3 experiments was approximately 10 ns. The pump and probe laser beams were lightly focused onto the sampling system, and the Raman light was collected using reflective optics into a spectrometer whose grating dispersed the light onto a liquid nitrogen cooled CCD detector. The Raman signal was acquired for 10−30 s by the CCD before reading out in the interfaced PC computer, and 10−30 scans of the signal were accumulated to produce a resonance Raman spectrum. The TR^3 spectra presented here were obtained by the subtraction of a resonance Raman spectrum with negative time delay of −100 ns (probe-before-pump spectrum) from the resonance Raman spectrum with a positive time delay (pump−probe spectrum). The TR^3 spectra in this work were calibrated by the known MeCN solvent's Raman bands with an estimated accuracy of ±5 cm^{-1}. A Lorentzian function was applied to integrate the relevant Raman bands to determine the decay and growth kinetics of the species observed in the experiments.

In the photolysis experiments, the sample solution was contained in a 10 mm UV cuvette and irradiated by an about 3.5 mW 266 nm unfocused laser beam from the fourth harmonic of a Nd:YAG laser. The absorption spectra of the photolyzed sample were acquired at a fixed time interval with a Perkin-Elmer Lambda 19 UV/vis spectrometer, and the absorption spectra for the ground-state sample solutions were acquired with a 10 mm UV grade cell using the same UV/vis spectrometer.

All of the geometry optimization, vibrational frequency, and TD-DFT calculations were done using the B3LYP and (U)B3LYP methods for the triplet state with a 6-31G* basis set. A Lorentzian function with a 15 cm^{-1} bandwidth was used with the Raman vibrational frequencies and relative intensities to obtain the calculated Raman spectra presented in this work. Frequency scaling factors were used in the comparison of the calculated results with the experimental results. All of the density functional theory calculations presented in this work made use of the Gaussian 98 program suite[22] operated on the High Performance Computing cluster (HPCPOWER) at the University of Hong Kong.

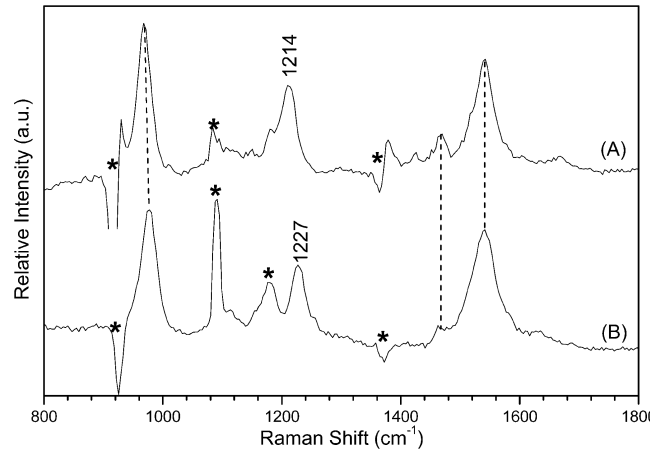

Figure 1. Transient resonance Raman spectra of ^{3}BP (A) and ^{3}SKP (B) obtained in MeCN solvent and acquired at 5 ns time delays between the pump (266 nm) and probe (319.9 nm) pulses. The asterisks mark regions affected by solvent subtraction artifacts and/or stray light.

Results and Discussion

1. TR^3 Spectra of SKP in Nonaqueous Solutions: Benzophenone-like Photochemistry. Except for the propionic acid chain, SKP has a structure similar to benzophenone, and thus SKP could be expected to exhibit benzophenone-like photochemistry in nonaqueous solutions. Figure 1B displays a 5 ns transient resonance Raman spectrum obtained after photolysis of (*S*)-ketoprofen (SKP) in MeCN. An overview of the TR^3 spectra obtained with a range of varying time delays after photolysis of SKP in MeCN is presented in Figure 1S of the Supporting Information. There are two species observed after 266 nm laser pulse photolysis of SKP in MeCN. The major species appearing at 5 ns and having its strongest bands at 973, 1227, and 1542 cm^{-1} is assigned to be the triplet ketoprofen (^{3}SKP) mainly due to two reasons. The first one is the sensitivity of the major species lifetime to the concentration of oxygen; when purged oxygen is used in the experiment, the major species decays within 100 ns, whereas it decays within 300 ns under open air conditions. This significant decrease in the lifetime of the major species indicates that the major intermediate observed is likely of triplet nature. The other reason is that the ^{3}SKP transient resonance Raman spectrum shows great similarity with the Raman features of the known transient triplet benzophenone (^{3}BP) that is shown in Figure 1A for comparison purposes. Examination of Figure 1 shows that the Raman spectrum of ^{3}SKP is very similar to that of the ^{3}BP spectrum with only a moderate difference in that the Raman feature at 1227 cm^{-1} for ^{3}SKP up-shifts about 13 cm^{-1} relative to the corresponding one at 1214 cm^{-1} for ^{3}BP. Most of the Raman bands observed in the TR^3 spectra of ^{3}SKP are due to vibrations associated with the C−C stretches and C−H bend motions, and more detailed assignments are listed in Table 1S in the Supporting Information. For example, the UB3LYP/6-31G* calculations predict the 1542 cm^{-1} Raman band is mainly due to the ring C−C stretching vibrational mode, the 1227 cm^{-1} Raman band is mostly due to a triplet carbonyl C−O stretch vibrational mode, and the 973 cm^{-1} Raman band is due to C−H bend motions in the nonsubstituted aromatic ring. The propionic acid chain in ^{3}SKP only causes some modest perturbations on the overall structure as compared to that of ^{3}BP whose optimized structure is given in Figure 2S of the Supporting Information. For example, as shown in Figure 2, the C−O bond length predicted from the UB3LYP/6-31G* calculations for the ^{3}SKP is 1.3293 Å, decreasing slightly as compared to the value of 1.3296 Å

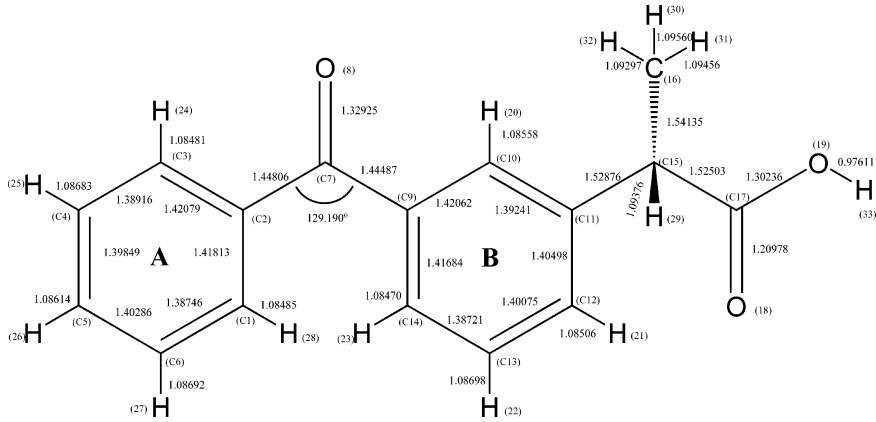

Figure 2. Optimized structure of ^{3}SKP obtained from UB3LYP/6-31G* calculations.

predicted for the same computations for ^{3}BP. This result is consistent with the C−O stretch Raman feature at 1227 cm^{-1} for ^{3}SKP up-shifting about 13 cm^{-1} relative to the corresponding one at 1214 cm^{-1} for ^{3}BP. In addition, the bonds lengths of C10−C11 and C11−C12 in the substituted aromatic ring for the ^{3}SKP are 1.3924 and 1.4050 Å, respectively, increasing slightly as compared to the corresponding bonds lengths of 1.3890 and 1.3986 Å, respectively, for ^{3}BP. These modest changes in the structure are consistent with the vibrational frequencies and experimental ns-TR^3 spectra of the two triplet species being very similar but not identical. Previous studies indicate the frequency of the C−O stretch mode appears in the 1400−1600 cm^{-1} range for a $\pi\pi^*$ nature triplet state and in the 1200−1400 cm^{-1} region for a typical nπ^* nature triplet state.[15,23−28] As illustrated above, the C−O stretching frequency for ^{3}SKP is located at 1227 cm^{-1}, and this indicates the ^{3}SKP has a nπ^* character configuration.

IPA is known to be a strong hydrogen donor solvent, so TR^3 were performed to see whether a hydrogen abstraction reaction will take place. In Figure 3, there are three transient species observed in the nanosecond-TR^3 spectra acquired following photolysis of SKP in neat IPA. The first species with its most intense bands at 977, 1095, 1231, and 1545 cm^{-1} has decayed noticeably at 5 ns and appears to be the same ^{3}SKP species probed in pure MeCN solvent (see Figure 1B). The second species has its most intense bands at 997, 1180, 1584 cm^{-1} and begins to grow in at time delays shorter than 5 ns and then decays to give a third species, which then decays on the hundreds of microseconds time-scale. This second species is thought to be the arylphenylketyl (ArPK) radical produced from the hydrogen abstraction of IPA by the ^{3}SKP species, which has a mostly nπ^* character. Figure 4 displays a comparison of the DFT calculated Raman spectrum for the ArPK radical with its structure displayed next to the spectrum (bottom) with the Raman spectra of the ArPK radical (middle) obtained at a time delay of 80 ns in Figure 3 and also to the TR^3 spectrum of an authentic diphenyl ketyl radical (top) obtained after 266 nm laser photolysis of BP in IPA.[15] The main experimental resonance Raman band positions and their assignments for the ArPK radical are listed in Table 1S. Examination of Figure 4 clearly shows that the TR^3 spectrum of the ArPK radical (middle) is very similar to that of the TR^3 spectrum of the diphenyl ketyl radical (top) with only some moderate frequency shifts. The TR^3 spectrum of the ArPK radical is also in good agreement with the DFT calculated Raman spectrum for the ArPK radical (bottom). This satisfactory agreement of the resonance Raman spectra clearly demonstrates that these spectra in Figure 4 are due to the same type of species, and

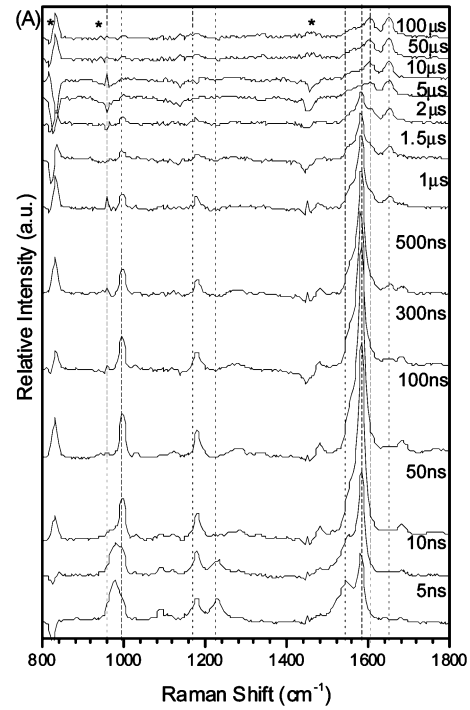

Figure 3. Ns-TR^3 spectra of ∼2 mM SKP in IPA obtained using a 266 nm pump excitation wavelength and a 319.9 nm probe wavelength at various time delays indicated next to the spectra.

the propionic acid chain in the ArPK radical only has limited perturbation on the structure and the properties on the ArPK radical as compared to the diphenyl ketyl radical. The detailed calculated DFT optimized structures for the ArPK radical and diphenyl ketyl radical are displayed in Figure 3S of the Supporting Information.

The ArPK radical has a growth time constant of ∼27 ns and a decay time constant of ∼780 ns under the experimental conditions employed here. The relatively short growth time implies that the ^{3}SKP is readily photoreduced by the hydrogen-donor IPA solvent to form the ArPK radical. The ArPK radical is likely to cross-couple with the dimethyl ketyl radical (DMK) formed from IPA at a *para*-position, which gives rise to the third species, 2-[3-(hydroxyl-(4-(2-hydroxypropan-2-yl)-cyclohexa-2,5-dienylidene)-methyl)-phenyl]-propanoic acid (*p*-ArPK-DMK), observed in ns-TR^3 spectra. This cross-coupling reaction is similar to the corresponding reaction observed for BP.[15] Figure 5 displays a comparison of the experimental ns-TR^3 spectrum at 100 μs obtained after photolysis of SKP in IPA (middle) to the calculated spectrum for the *p*-ArPK-DMK species (bottom)

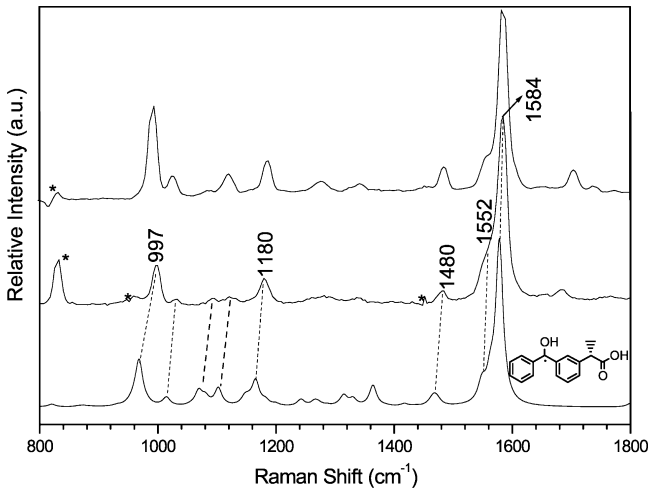

Figure 4. Comparison of experimental ns-TR^3 spectrum obtained after photolysis of SKP in neat IPA acquired at a time delay of 80 ns (middle) with the DFT calculated spectrum for the ArPK radical with its structure displayed next to the spectrum (bottom) and the TR^3 spectrum of an authentic diphenyl ketyl radical (top) obtained after 266 nm laser photolysis of BP in IPA.[15] The asterisks (*) mark regions affected by solvent subtraction artifacts and/or stray light.

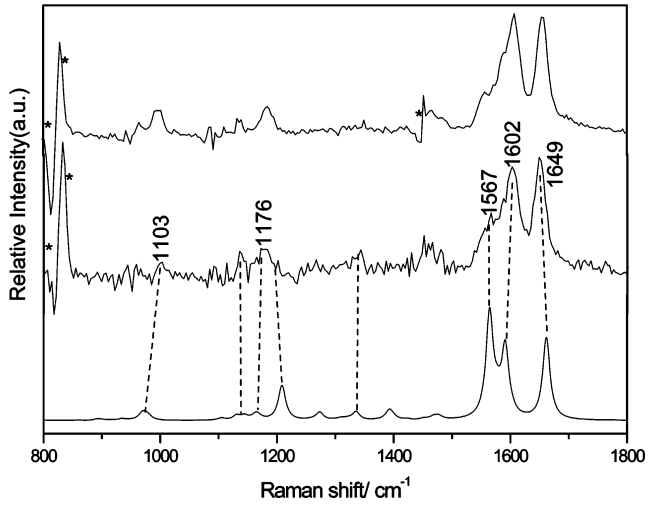

Figure 5. Comparison of experimental ns-TR^3 spectrum by photolysis of SKP in neat IPA acquired at time delay of 100 μs (middle), with the DFT calculated spectrum for *p*-ArPK-DMK (bottom), and the TR^3 spectrum of the analogous cross-coupling species obtained by photolysis of BP in IPA (top) and reported in ref 15. The asterisks mark regions affected by solvent subtraction artifacts and/or stray light.

and also to the TR^3 spectrum of the analogous cross-coupling species obtained by photolysis of BP in IPA (top).[15] Inspection of Figure 5 shows that the calculated *p*-ArPK-DMK spectrum exhibits reasonable agreement with the experimental spectrum. Moderate discrepancies in the relative Raman intensity pattern were found for *p*-ArPK-DMK, and this can be explained by the experimental Raman spectrum being resonantly enhanced while the calculated one is a nonresonant Raman spectrum. Figure 5 also shows that the *p*-ArPK-DMK TR^3 spectrum (middle) is very similar to the TR^3 spectrum of the corresponding cross-coupling product produced (top) from the analogous reaction of BP in IPA,[15] and this indicates that the propionic acid side chain does not substantially affect the cross-coupling reaction product structure associated with the chromophore.

The ^{3}SKP species also demonstrates its hydrogen abstraction ability in neat MeCN. There is a weak species observed with its strongest band at 1584 cm^{-1} appearing after 20 ns (see Figure 1S in the Supporting Information), and it is thought to be due to the hydrogen abstraction either from a water impurity or with SKP itself. Because this minor species was not observed in the BP case,[15] the explanation of hydrogen abstraction from the water impurity appears less likely. The minor species should therefore be more likely from either intermolecular or intramolecular hydrogen abstraction among the SKP molecules present in the reaction system. To verify this, TR^3 experiments using two different concentrations of SKP were done. The changes in the TR^3 spectra intensities were determined using integration of the area of the 1584 cm^{-1} Raman band, and these intensity changes could be adequately fitted via a two-exponential function. The growth time constant for this minor species in the TR^3 experiments using ~2 mM SKP in pure MeCN is 46 ns, while that using a ~4 mM concentration is 32 ns. The lack of strong concentration dependence in the growth time constant suggests that the intermolecular hydrogen abstraction among SKP molecules is unlikely to take place appreciably so the weak species might arise mostly from the intramolecular hydrogen abstraction of the side chain moiety. The clear identification of the weak species is difficult due to the weak intensity of only one clear fingerprint band at 1584 cm^{-1}.

2. TR^3 Spectra of SKP in Aqueous Solutions: pH-Dependent Photochemistry. The UV/vis spectra of the ground state of SKP in several solvents were obtained (see Figure 6S in the Supporting Information) and show that the strongest absorption band is at ~254 nm in the MeCN, IPA, 1:1 MeCN:H_2O, and 1:1 MeCN:$HCl_{(aq)}$ solvents (this band is due to the undissociated acid molecule that is predominant in these solutions), while the absorption band is blue-shifted as the relative amount of the conjugate base increases as shown in the spectra obtained in the 1:1 MeCN:16.4 mM $NaOH_{(aq)}$ and 3:7 MeCN:PBS solvents. This seems to suggest that the ground-state SKP determines most of its photochemistry outcome as previously suggested by several research groups.[9,14]

2.1. TR^3 Spectra of SKP in 1:1 MeCN:Pure Water and 1:1 MeCN:Acidic Solution Exhibit Photochemistry Similar To That Found in Nonaqueous Solvent. The photochemistry of SKP in 1:1 MeCN:H_2O and 1:1 MeCN:$HCl_{(aq)}$ is very similar to that observed in IPA. The TR^3 spectra of ~2 mM SKP in 1:1 MeCN:H_2O and 1:1 MeCN:$HCl_{(aq)}$ are presented in Figures 4S and 5S of the Supporting Information. After photolysis of SKP in these two aqueous solutions, ^{3}SKP was generated first, and ^{3}SKP decays within 100 ns to form the ArPK radical. The TR^3 spectrum acquired at 800 ns after photolysis of SKP in 1:1 MeCN:$HCl_{(aq)}$ solvent was compared to that of SKP in neat IPA acquired at 600 ns in Figure 6. There is a fairly good agreement in the Raman shift frequencies between the spectra of the second species obtained in 1:1 MeCN:$HCl_{(aq)}$ and ArPK radical obtained in IPA. This suggests that the second species may be the ArPK radical. To further determine if the species acquired at 800 ns observed under acidic conditions is a carbocation or a ArPK-like species, TR^3 experiments using the carbocation quencher Cl^- and an acidic solution of $HClO_4$ in which the ClO_4^- ions are of relatively high stability and will not quench carbocation were carried out on the same day. Kinetics plots of the data obtained under the two different conditions, ~2 mM SKP in 1:1 MeCN:0.1 M $HCl_{(aq)}$ and 1:1 MeCN:0.1 M $HClO_{4(aq)}$, were obtained by fitting the areas under the strongest band at 1584 cm^{-1} against time using a two-exponential function. These results show that the growth time constant is 60 ns and the decay time constant is approximately 800 ns in both cases. This in turn implies the species acquired at 800 ns may not bear a

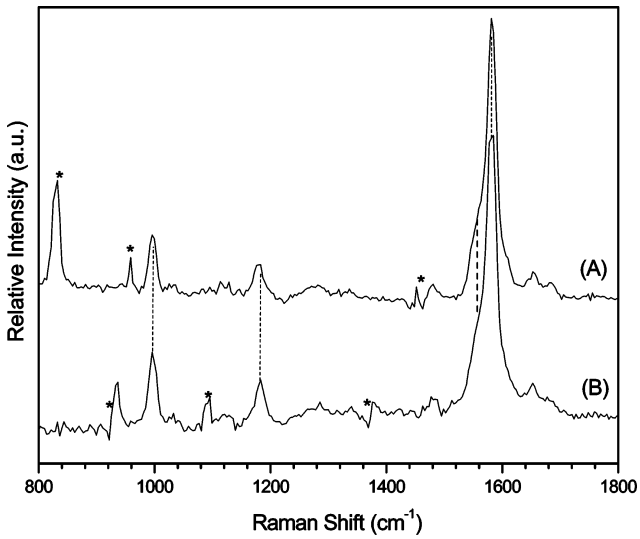

Figure 6. Comparison of the spectra of (A) ~2 mM SKP in 1:1 MeCN:$HCl_{(aq)}$ acquired at a 800 ns time delay with the spectrum (B) ~2 mM SKP acquired in neat IPA at a time delay of 600 ns.

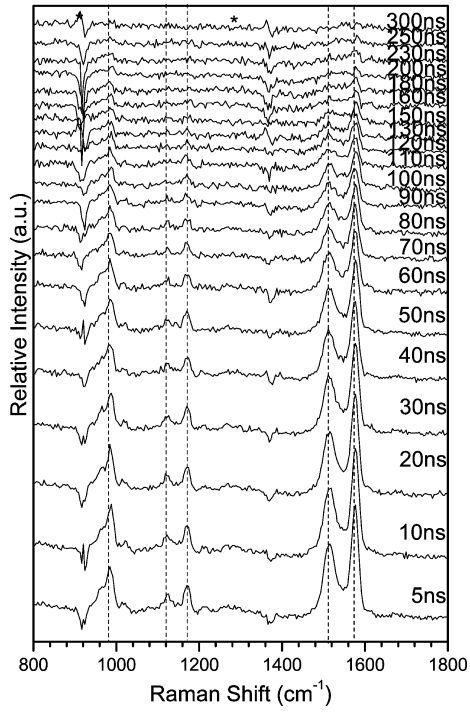

Figure 7. Ns-TR^3 spectra of ~2 mM SKP in a 1:1 MeCN:16.4 mM $NaOH_{(aq)}$ solution obtained using a 266 nm pump excitation wavelength and a 319.9 nm probe wavelength at various time delays indicated next to the spectra. The asterisk (*) marks regions affected by solvent subtraction artifacts and/or stray light.

significant positive charge and is more likely to be a species that resembles the structure of the ArPK radical.

The ArPK radical is thought to arise from ^{3}SKP, which may involve the participation of water molecules. Besasson and Gramain used an indirect approach to determine the quantum yield for ketyl radical formation and the rate constant of hydrogen abstraction exhibited by BP in pure H_2O using various lactams in both MeCN and H_2O solvents.[29] They proposed that hydrogen abstraction from the poor hydrogen donor H_2O can be achieved by the triplet BP. Because the neutral form of SKP is predominant in the 1:1 MeCN:H_2O solvent, SKP is expected to demonstrate a reactivity similar to that of BP. Two sets of TR^3 experiments using ~2 mM SKP in 1:1 MeCN:H_2O and

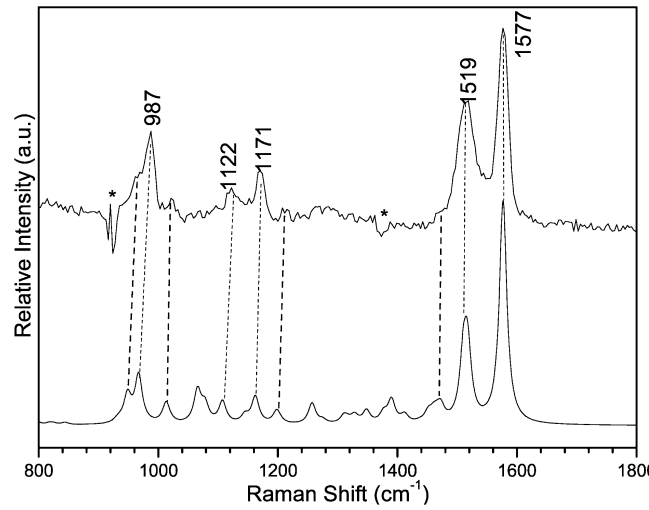

Figure 8. Comparison of the experimental ns-TR^3 spectrum of SKP in a 1:1 MeCN:16.4 mM $NaOH_{(aq)}$ solution acquired at time delay of 10 ns (top), with the DFT calculated spectrum for the ^{3}BCH (bottom) whose optimized structure from DFT calculations is shown in Figure 9. The asterisk (*) marks regions affected by solvent subtraction artifacts and/or stray light.

1:1 MeCN:D_2O were performed on the same day to ensure the laser conditions were maintained nearly constant. The kinetics study under these conditions were carried out by fitting the areas under the 1584 cm^{-1} Raman band by a two-exponential function at different time delays, and this found that the growth time constant for ArPK radical in 1:1 MeCN:H_2O is 100 ns whereas that in 1:1 MeCN:D_2O is 204 ns. A typical primary kinetics isotope effect of $k_D/k_H = 2$ was observed. This implies the O−H bond cleavage is involved in the rate-determining step in the formation of the ArPK radical; yet the mechanism of how water molecules participate remains unclear due to its poor hydrogen-donating property and the instability of the hydroxy radical. The decay of the ArPK radical is faster in D_2O than in H_2O; whether or not this is a consequence of a deuterated hydroxyl radical being more reactive remains uncertain, and more work will be needed in an attempt to better explain this observation.

A new species is observed after the decay of the ArPK radical, which may form from the self-coupling between ArPK radical or the cross-coupling with water molecules. Different concentrations and pump power conditions were used for the TR^3 experiments to obtain kinetics plots of the ArPK radical in which its decay time constant could be associated with the growth time constant of the new species. Kinetics plots of the 1584 cm^{-1} band were obtained, but no concentration or power dependence in the decay time constant was observed as illustrated in Figure 7S in the Supporting Information. This implies that the third species does not arise from self-coupling among ArPK radicals. Instead, it is more likely to couple with the surrounding water molecules, which are present in large excess. The calculated spectrum for the cross-coupled species (2*S*)-2-[3-(hydroxyl-(4-hydroxycyclohexa-2,5-dienylidene)-methyl)-phenyl]-propanoic acid (denoted as *p*-OH) using the B3LYP/6-31G* level of theory shows reasonable agreement with the TR^3 Raman frequencies observed in the experimental spectrum in Figure 8S and Table 1S.

2.2. TR^3 Spectra of SKP in 1:1 MeCN:Alkaline and 3:7 MeCN:PBS Aqueous Solutions: Observation of the Protonated Biradical Carbanion. Photoinduced decarboxylation was found to be an efficient and general reaction for different types of arylcarboxylic acids in aqueous solution at pH > pK_a.[30] Figure 7 displays ns-TR^3 spectra of ~2 mM SKP in 1:1 MeCN:16.4

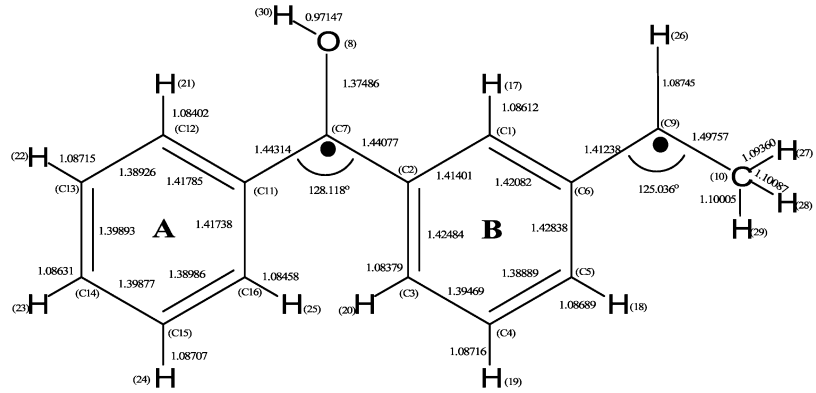

Figure 9. Optimized structure for the ^{3}BCH species obtained from B3LYP/6-31G* calculations.

TABLE 1: Excited-State Energies and Oscillator Strength from TD-DFT ((U)B3LYP/6-31G*) Calculations for ^{3}BCH

excited state	transition energy (nm)	oscillator strength
1	438	0.1101
2	387	2.4×10^{-3}
3	366	9×10^{-4}
4	354	1.7×10^{-3}
5	346	1.4×10^{-3}
6	321	0.0835
7	320	0.0498
8	318	0.2049
9	303	0.1109
10	302	3.24×10^{-3}

mM $NaOH_{(aq)}$ with time delays indicated next to each spectrum. Inspection of Figure 7 shows that only one species is seen in the TR^3 spectra under these conditions. The strongest Raman bands are observed at 987, 1517, and 1577 cm^{-1}, and two less intense Raman bands are seen at 1122 and 1171 cm^{-1}; the main experimental resonance Raman band positions and the descriptions of the bands are listed in Table 1S. Oxygen purge experiments were performed, and plots of the integrated areas for the strongest band at 1577 cm^{-1} as a function of time delays from 5 to 150 ns were obtained. The species was found to be sensitive to oxygen and has its lifetime shortened from 130 $\pm$ 10 to 58 $\pm$ 10 ns. This intermediate is therefore believed to have triplet character. It has been suggested by Eriksson and co-workers[14] that a prompt decarboxylation of the triplet conjugate base of ketoprofen takes place to produce a carbanion in which its biradical form is the more stable resonance structure, and hence the carbanion should have more biradical character. It was then suggested by Borsarelli and co-workers[12] that protonation of the biradical carbanion (^{3}BC$^-$) takes place at pH = 6.1. Therefore, the photodecarboxylation of SKP seems to be a triplet state process. This process is different from decarboxylation of *o*-acetylphenyl-acid, which starts from the highly excited singlet state with charge-transfer character.[31] This could possibly be due to the acid chain of *o*-acetylphenyl-acid being much closer to the carboxyl group, which leads to the intramolecular proton transfer to the carboxyl group easily in the $\pi\pi^*$ state. Examination of the kinetics plots and the possibility that the observed species could be either ^{3}BC$^-$ or a protonated biradical carbanion (^{3}BCH) was investigated. Calculations predicting the total energy, the optimized geometry, and vibrational frequencies for both species were performed. The experimental 10 ns TR^3 spectrum is in good agreement with the B3LYP/6-31G* calculated Raman spectrum for the protonated biradical anion (denoted as ^{3}BCH) as shown in Figure 8. This suggests the species observed in Figure 7 can be tentatively assigned to the protonated biradical anion (^{3}BCH) with the calculated optimized structure shown in Figure 9. Selected vibrational modes associated with the observed Raman frequencies are presented in Table 1 and compared to the corresponding calculated vibrational frequencies for the ^{3}BCH species. Most of the Raman bands observed for the ^{3}BCH species are due to the vibrations associated with the C−C stretch motions of the phenyl rings. For example, the Raman bands at 987, 1122, 1517, and 1577 cm^{-1} are mainly due to these kinds of vibrational modes. The Raman band at 1171 cm^{-1} has contributions not only from the C−C stretch motions, but also from an O−H bend motion. The calculated optimized structure in Figure 9 for the ^{3}BCH species reveals a delocalization of the radical electrons into the aromatic ring, making the C−C bond length change to become about 1.4 Å, which stabilizes the triplet state.

TD-DFT calculations were also done for the triplet biradical carbanion and the ^{3}BCH species to further verify the assignment of the species observed in the TR^3 spectra. The TD-DFT calculation results show that ^{3}BCH has a larger oscillator strength near the probe laser wavelength, whereas the absorption spectrum of ^{3}BC$^-$ shows a relatively weak oscillator strength near the probe laser wavelength used in the experiments. Table 1 shows the excited energies and oscillator strength for ^{3}BCH, which suggests the transient species observed in ns-TR^3 spectra is more likely to be the ^{3}BCH species.

Ns-TR^3 experiments of ~2 mM SKP in 3:7 MeCN:PBS were carried out to mimick physiological conditions (pH = 7.4) in an attempt to better understand the photochemical pathway for SKP under such conditions. These TR^3 spectra are provided in Figure 10S of the Supporting Information. The ^{3}BCH species was also observed in the 3:7 MeCN:PBS solution. A kinetics plot of the 1577 cm^{-1} band intensity characteristic of the ^{3}BCH species was obtained by fitting its integrated areas as a function of time by a two-exponential function. The fitted results show that the growth time constant is ~18 ns, whereas the decay time constant is ~411 ns. Both have longer times than that observed

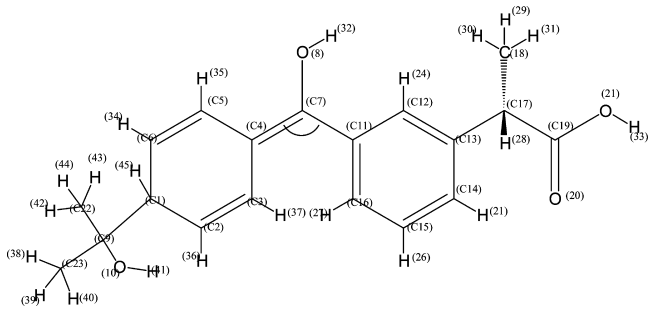

Figure 10. *p*-ArPK-DMK with atom numbers.

TABLE 2: Selected Bond Length (Å) Parameters for Some Species Observed in the Photochemistry of SKP and BP

	^{3}BP	^{3}SKP	DPK	ArPK	*p*-DPK-DMK	*p*-ArPK-DMK
C1−C2	1.4028	1.4029	1.4000	1.3988	1.5077	1.5081
C2−C3	1.3875	1.3875	1.3891	1.3896	1.3444	1.3442
C3−C4	1.4184	1.4181	1.4181	1.4172	1.4613	1.4623
C4−C5	1.4210	1.4208	1.4193	1.4183	1.4619	1.4623
C5−C6	1.3890	1.3892	1.3908	1.3889	1.3444	1.3453
C1−C6	1.3986	1.3985	1.3973	1.3991	1.5070	1.5065
C4−C7	1.4465	1.4481	1.4465	1.4414	1.3665	1.3711
C7−C11	1.4465	1.4449	1.4392	1.4438	1.4763	1.4747
C7−O8	1.3296	1.3293	1.3748	1.3738	1.3821	1.3771
C11−C12	1.4210	1.4206	1.4187	1.4215	1.4093	1.4067
C12−C13	1.3890	1.3924	1.3894	1.3956	1.3934	1.3961
C13−C14	1.3896	1.4050	1.3990	1.4055	1.3963	1.4030
C14−C15	1.4028	1.4008	1.3994	1.3975	1.3970	1.3944
C15−C16	1.3875	1.3872	1.3887	1.3894	1.3933	1.3934
C11−C16	1.4184	1.4168	1.4193	1.4170	1.4075	1.4049

SCHEME 2: Proposed Partial Mechanism for the Dual-Photochemistry of SKP Consistent with the TR^3 Results[a]

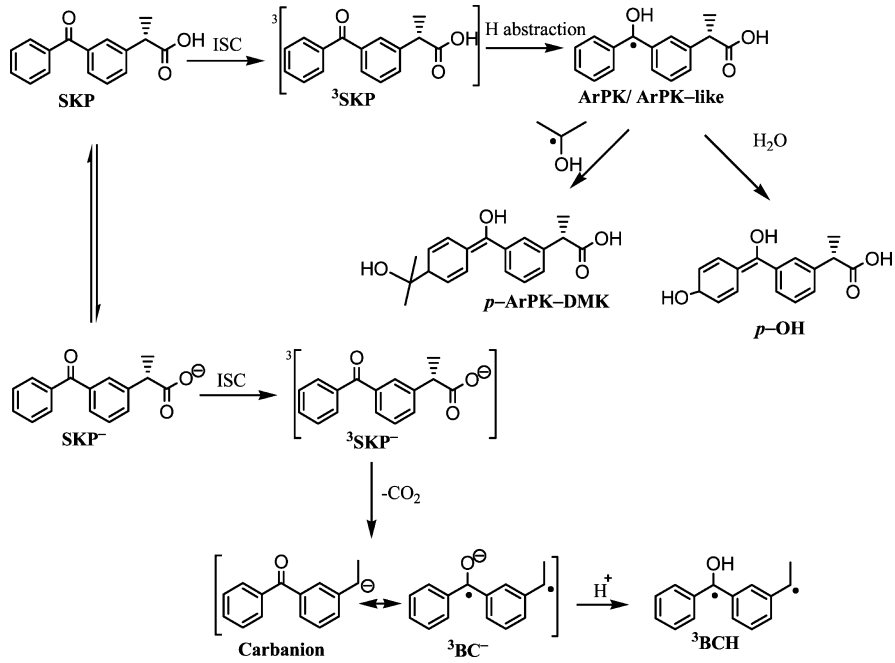

[a] Note the scheme only shows part of the overall mechanisms and focuses mainly on species observed in the TR^3 spectra.

in the 1:1 MeCN:16.4 mM $NaOH_{(aq)}$ case, in which the ^{3}BCH species accumulates to its maximum within 5 ns and decays with a time constant of about 130 ns. This phenomenon may be accounted for by the relatively strong ionic strength of PBS that can stabilize the negatively charged species $^3BC^-$, which therefore gives a relatively longer growth time constant, whereas the shorter lifetime of ^{3}BCH in strongly alkaline solution may be due to the carbocation-like radical sites being readily attacked by OH^-.

3. Comparison of Some Properties of Intermediates Observed in the Photochemistry of Benzophenone and Ketoprofen. The photochemistry of SKP in MeCN, IPA, and 1:1 MeCN:pure water solvents exhibits a great degree of similarity with benzophenone (BP). Both of them are excited by a $\pi\pi^*$ transition from S_1 to S_n, which then undergo fast intersystem crossing to form T_2 with a $\pi\pi^*$ character. Internal conversion then takes place to become a T_1 state of $n\pi^*$ nature with hydrogen abstraction ability. Hydrogen abstraction of the triplet state of SKP occurs to form a ketyl radical-like species in MeCN from the side chain of its molecule, while only the triplet BP was observed in MeCN by Phillips and co-workers.[15] Hydrogen abstraction ability of the triplet SKP is similar to the triplet BP in IPA. The triplet SKP abstracts a hydrogen atom from the IPA to form a radical ArPK and IPA becomes DMK. ArPK radical and DMK couple to form the third transient species in a manner similar to how DPK and DMK did in the case of BP.[15]

The propionic acid chain substituted in the SKP only results in some moderate difference for the structures of the ^{3}SKP, ArPK, and *p*-ArPK-DMK species as compared to their parent benzophenone analogous species. Figure 10 and Table 2 display some parameters for the optimized geometries of the species of interest. Examination of Figure 10 and Table 2 shows that the influence of the propionic acid substitution mainly occurs at the substituted aromatic ring and has only a slight effect on the unsubstituted aromatic ring. These differences in the structures of SKP and BP species only result in some moderate difference in their properties. Figures 11S−13S in the Supporting Information display the HOMO and LUMO diagrams for the transient species of the BP and SKP reactions. These results indicate that the triplet BP and SKP have similar electron density changes upon going from the triplet to the ketyl radical. For ArPK, there is a change in the electron density in the acid side chain upon going from the HOMO to the LUMO. Examination

of the HOMO and LUMO diagrams shows that both *p*-DPK-DMK and *p*-ArPK-DMK have enol and cyclohexadienyl character. This indicates that the photochemical reactivity of SKP resembles that of BP and the reactive center is mainly associated with the carbonyl group and the unsubstituted aromatic ring.

The TR^3 experiments for SKP in the aqueous solution containing 0.1 M $HClO_4$ and 0.1 M HCl were also done, and photochemistry similar to that in IPA or pure water mixed solution was observed. This result is different from the behavior of BP in the acidic aqueous solution. A hydration species was observed after photolysis of BP in the 1:1 MeCN:0.1 M $HClO_4$ solution.[32] This indicates that the excited triplet of BP is easy to be protonated.[33] Here, the propionic acid chain substitution in SKP appears to modify the reactivity of ^{3}SKP toward a proton, and it is necessary to do some more detailed work in more acidic aqueous solution to more clearly characterize the reactivity of the ^{3}SKP species.

Interestingly, SKP shows a very different photochemical behavior as compared to that of BP in the PBS solution and strong basic solution. The TR^3 experiments for SKP in a strong basic solution indicate that the initial stage of SKP phototoxicity involves the formation of the triplet state anionic species by intersystem crossing (ISC) from the deprotonated first singlet state. A decarboxylation reaction will then occur to produce the carbanion structure and its resonance form ($^3BC^-$). $^3BC^-$ is easily protonated at the anionic oxygen to form a neutral triplet ^{3}BCH. This species can last for several microseconds in PBS solution. However, the photochemistry of BP in a basic solution is almost the same as in the neutral aqueous solution. This gives us an important vibrational fingerprint identification of the long-lived reactive species of SKP photochemistry likely to react with biological components and insight to better understand how KP may induce phototoxicity. A recent time-resolved absorption (TA) study[6] of the photolysis of KP in a phosphate buffer solution of pH 7.4 also observed the fast formation of an intermediate that had a microsecond lifetime and was tentatively assigned to the protonated form of a triplet carbanion species like ^{3}BCH. Our present TR^3 results under similar conditions provide strong confirmation that the species observed in the TA experiments is ^{3}BCH. The TA study also observed that this intermediate can be quenched by histidine (His), and it was determined that it was the protonated form, $HisH^+$, that reacted with the intermediate with a close to diffusion-controlled rate constant.[6] While the photoreaction of KP with a protein has been examined by several groups using TA spectroscopy,[4,34−37] the TA spectra are complicated due to spectral overlap of the transient species like the ketyl radical (ArPK) and ^{3}BCH whose TA spectra are similar to one another, and this makes it difficult to unravel the reactions taking place. The TR^3 spectra observed here for ArPK and ^{3}BCH demonstrate that these vibrational spectra can be used to readily tell these species apart from one another. This suggests that further TR^3 studies of the photochemistry of KP in different environments such as proteins should prove useful to help unravel the complex reactions observed in proteins and other biological systems. We note that the decarboxylation reaction was not observed in our study here and must occur on time-scales faster than the ~5 ns resolution of the TR^3 experiments reported here.

Conclusion

The photochemistry of (*S*)-ketoprofen (SKP) was studied using ns-TR^3 and in conjunction with results from DFT calculations. The form of the species of the ground state of SKP is important for determining which photochemical pathway will be taken after photoexcitation, either benzophenone-like photochemistry or degradation via a decarboxylation. Scheme 2 displays a summary of a proposed partial mechanism for SKP that is consistent with the species observed in the TR^3 spectra.

SKP in neat MeCN, IPA, 1:1 MeCN:H_2O, and 1:1 MeCN:$H^+_{(aq)}$ solutions in which SKP is mainly in its neutral or undissociated form exhibit benzophenone-like photochemistry in which a triplet state with nπ^* nature is formed via intersystem crossing. This triplet state has a shorter lifetime in IPA and aqueous solution and exhibits a hydrogen abstracting chemical reactivity that readily undergoes photoreduction by the hydrogen donor solvent to form a ketyl radical (ArPK). A D_2O experiment was carried out and found a slower formation of the ArPK species by a factor of 2. This implies the involvement of O−H bond breakage in the formation of ArPK. ArPK then cross-couples with DMK and H_2O molecules at its *para*-position to form relatively long-lived transient species, *p*-ArPK-DMK and *p*-OH, respectively. The same concentrations of $HCl_{(aq)}$ and $HClO_{4(aq)}$ were used to identify the ArPK radical for which Cl^- is a carbocation quencher. The lifetime of the ArPK-like species does not have a significant decrease in its lifetime when Cl^- is added, which suggests a lack of a positive charge character in the ArPK-like species. A ketyl radical-like species was also found in the neat MeCN solvent, but the concentration independence of this process indicates that it is an intramolecular hydrogen abstraction rather than an intermolecular hydrogen abstraction among SKP molecules.

Only one species was observed in the ns-TR^3 experiments using a 319.9 nm probe wavelength after 266 nm photolysis of SKP in 1:1 MeCN:OH^- and 3:7 MeCN:PBS solutions where its conjugate base is the predominant species. This transient species was found to be sensitive to the concentration of O_2, which suggests it likely has triplet character. This species was tentatively assigned to the protonated biradical carbanion ^{3}BCH on the basis of a comparison of the experimental TR^3 spectrum to that predicted by DFT calculations for the Raman spectrum of this species. The TR^3 experiments for SKP in a strong basic solution suggest that the early steps of SKP phototoxicity involve the formation of the triplet state anionic species by intersystem crossing (ISC) from the deprotonated first singlet state, and then a decarboxylation reaction takes place to form the carbanion structure and its resonance form ($^3BC^-$). $^3BC^-$ is readily protonated at the anionic oxygen to produce a neutral triplet ^{3}BCH that has a lifetime of several microseconds in PBS solution. In contrast, the photochemistry of BP in a basic solution is almost the same as in the neutral aqueous solution. The TR^3 results here provide an important vibrational fingerprint identification of the long-lived reactive species of SKP photochemistry that are likely to react with biological components and hence provide new insight to better understand how KP can induce phototoxicity. We note that a recent time-resolved absorption (TA) study[6] of the photolysis of KP in a phosphate buffer solution of pH 7.4 also observed the very quick formation of an intermediate tentatively assigned to the protonated form of a triplet carbanion species like ^{3}BCH that had a microsecond lifetime in good agreement with our present TR^3 results under similar conditions. The TR^3 results here provide strong confirmation that the species seen in the TA experiments is ^{3}BCH. While the photoreaction of KP with a protein has been examined by several groups using TA spectroscopy,[4,34−37] the TA spectra are complicated due to spectral overlap of the transient species like the ketyl radical (ArPK) and ^{3}BCH whose TA spectra are similar to one another, which complicates determining which

main reactions occur. The TR^3 spectra seen here for ArPK and ^{3}BCH show that these vibrational spectra can be employed to easily distinguish these species from one another and suggest that further TR^3 studies of the photochemistry of KP in different environments like proteins should be helpful to better elucidate the complex reactions observed in proteins and other biological systems.

Acknowledgment. This work was supported by a grant from the Research Grants Council of Hong Kong (HKU 7035/08P), the award of a Croucher Foundation Senior Research Fellowship (2006−07) from the Croucher Foundation, and an Outstanding Researcher Award (2006) from the University of Hong Kong to D.L.P.

Supporting Information Available: Figure 1S: Ns-TR^3 spectra of ~2 mM SKP in neat MeCN obtained using 266 nm pump excitation wavelength and 319.9 nm probe wavelength at various time delays, which were indicated next to the spectra at open air. Figure 2S: Optimized structure of the triplet benzophenone. Figure 3S: Optimized structure for ArPK radical and the diphenyl ketyl radical. Figure 4S: ns-TR^3 spectra of ~2 mM SKP in 1:1 MeCN:H_2O obtained using 266 nm pump excitation wavelength and 319.9 nm probe wavelength at various time delays, which were indicated next to the spectra. Figure 5S: ns-TR^3 spectra of ~2 mM SKP in 1:1 MeCN:$HCl_{(aq)}$ of pH = 3 obtained using 266 nm pump excitation wavelength and 319.9 nm probe wavelength at various time delays, which were indicated next to the spectra. Figure 6S: Comparison of absorption spectra of SKP in different solvents. Figure 7S: ns-TR^3 spectra of (A) ~2 mM SKP in 1:1 MeCN:H_2O acquired using relatively low pump power conditions, (B) ~2 mM SKP in 1:1 MeCN:H_2O acquired using relatively high pump laser power, and (C) ~4 mM SKP in 1:1 MeCN:H_2O with their time delays indicated next to the spectra and their corresponding kinetics plots of 1584 cm^{-1}. Figure 8S: Comparison of experimental ns-TR^3 spectrum of SKP in 1:1 MeCN:H_2O acquired at a time delay of 15 μs (top), with the DFT calculated spectrum for species with optimized structure shown in Figure 9S (bottom). Figure 9S: Optimized structure of *p*-OH. Table 1S lists the Raman frequencies (cm^{-1}) and assignments for *p*-OH where the structural labels are those shown in Figure 9S. Figure 10S: ns-TR^3 spectra of ~2 mM SKP in 3:7 MeCN:PBS obtained using a 266 nm pump excitation wavelength and a 319.9 nm probe wavelength at various time delays, which were indicated next to the spectra. Figure 11S: Simple schematic diagrams showing the electron density for the HOMO and LUMO associated with the strongest absorption transition for triplet BP and triplet SKP predicted from TD-DFT calculation. Figure 12S: Simple schematic diagrams showing the electron density for the HOMO and LUMO associated with the strongest absorption transition for DPK and ArPK predicted from TD-DFT calculation. Figure 13S: Simple schematic diagrams showing the electron density for the HOMO and LUMO associated with the strongest absorption transition for *p*-DPK-DMK and *p*-ArPK-DMK predicted from TD-DFT calculation. Figure 14S: Cartesian coordinates, total energies, and vibrational zero-point energies for the optimized geometries obtained from the (U)B3LYP/6-31G** calculations for the related transient species. This material is available free of charge via the Internet at http://pubs.acs.org.

References and Notes

(1) Ljunggren, B. *Photodermatology* **1985**, *2*, 3–9.
(2) Przybilla, B.; Schwab-Przybilla, U.; Ruzicka, T.; Ring, J. *Photodermatology* **1987**, *4*, 73–78.
(3) Lukeman, M.; Scaiano, J. C. *J. Am. Chem. Soc.* **2005**, *127*, 7698–7699.
(4) Montis, S.; Manet, I.; Manoli, F.; Morrone, R.; Nicolosi, G.; Sortino, S. *Photochem. Photobiol.* **2006**, *84*, 13–19.
(5) Suzuki, H.; Suzuki, T.; Ichimura, T.; Ikesue, K.; Sakai, M. *J. Phys. Chem. B* **2007**, *111*, 3062–3068.
(6) Suzuki, T.; Okita, T.; Osanai, Y.; Ichimura, T. *J. Phys. Chem. B* **2008**, *112*, 15212–15216.
(7) Montis, S.; Sortino, S.; De Guidi, G.; Marconi, G. *J. Chem. Soc., Faraday Trans.* **1997**, *93*, 2269–2275.
(8) Boscá, F.; Miranda, M. A.; Carganico, G.; Mauleon, D. *Photochem. Photobiol.* **1994**, *60*, 96–101.
(9) Martínez, L. J.; Scaiano, J. C. *J. Am. Chem. Soc.* **1997**, *119*, 11066–11070.
(10) Cosa, G.; Martinez, L. J.; Scaiano, J. C. *Phys. Chem. Chem. Phys.* **1999**, *1*, 3533–3537.
(11) Laferrière, M.; Sanrame, C. N.; Scaiano, J. C. *Org. Lett.* **2004**, *6*, 873–875.
(12) Borsarelli, B. C.; Braslavsky, S.; Sortino, E. S.; Marconi, G.; Monti, S. *Photochem. Photobiol.* **2000**, *72*, 163–171.
(13) Boscá, F.; Marin, M. L.; Mirada, M. A. *Photochem. Photobiol.* **2001**, *74*, 637–655.
(14) Musa, K. A. K.; Matxain, J. M.; Erikkson, L. A. *J. Med. Chem.* **2007**, *50*, 1735–1743.
(15) Du, Y.; Ma, C.; Kwok, W. M.; Xue, J.; Phillips, D. L. *J. Org. Chem.* **2007**, *72*, 7148–7156.
(16) Xue, J.; Du, Y.; Guan, X.; Guo, Z.; Phillips, D. L. *J. Phys. Chem. A* **2008**, *112*, 11582–11589.
(17) Du, Y.; Xue, J.; Ma, C.; Kwok, W. M.; Phillips, D. L. *J. Raman Spectrosc.* **2008**, *39*, 503–514.
(18) Xue, J.; Chan, P. Y.; Du, Y.; Guo, Z.; Chung, C. W. Y.; Toy, P. H.; Phillips, D. L. *J. Phys. Chem. B* **2007**, *111*, 12676–12684.
(19) Du, Y.; Guan, X.; Kwok, W. M.; Chu, L. M.; Phillips, D. L. *J. Phys. Chem. A* **2005**, *109*, 5872–5882.
(20) Chan, P. Y.; Ong, S. Y.; Zhu, P.; Zhao, C.; Phillips, D. L. *J. Phys. Chem. A* **2003**, *107*, 8067–8074.
(21) Zhu, P.; Ong, S. Y.; Chan, P. Y.; Leung, K. H.; Phillips, D. L. *J. Am. Chem. Soc.* **2001**, *123*, 2645–2649.
(22) Frisch, M. J.; Trucks, G. W.; Schlegel, H. B.; Scuseria, G. E.; Robb, M. A.; Cheeseman, J. R.; Zakrzewski, V. G.; Montgomery, J. A., Jr.; Stratmann, R. E.; Burant, J. C.; Dapprich, S.; Millam, J. M.; Daniels, A. D.; Kudin, K. N.; Strain, M. C.; Farkas, O.; Tomasi, J.; Barone, V.; Cossi, M.; Cammi, R.; Mennucci, B.; Pomelli, C.; Adamo, C.; Clifford, S.; Ochterski, J.; Petersson, G. A.; Ayala, P. Y.; Cui, Q.; Morokuma, K.; Malick, D. K.; Rabuck, A. D.; Raghavachari, K.; Foresman, J. B.; Cioslowski, J.; Ortiz, J. V.; Baboul, A. G.; Stefanov, B. B.; Liu, G.; Liashenko, A.; Piskorz, P.; Komaromi, I.; Gomperts, R.; Martin, R. L.; Fox, D. J.; Keith, T.; Al-Laham, M. A.; Peng, C. Y.; Nanayakkara, A.; Gonzalez, C.; Challacombe, M.; Gill, P. M. W.; Johnson, B.; Chen, W.; Wong, M. W.; Andres, J. L.; Gonzalez, C.; Head-Gordon, M.; Replogle, E. S.; Pople, J. A. *Gaussian 98*, revision A.7; *Gaussian 03*, revision B.05; Gaussian, Inc.: Pittsburgh, PA, 1998; 2003.
(23) Webb, S. P.; Yeh, S. W.; Phillips, L. A.; Tolbert, L. M.; Clark, J. H. *J. Am. Chem. Soc.* **1984**, *106*, 7286–7288.
(24) Webb, S. P.; Phillips, L. A.; Yeh, S. W.; Tolbert, L. M.; Clark, J. H. *J. Phys. Chem.* **1986**, *90*, 5154–5164.
(25) Schwartz, B. J.; A., P. L.; Harris, C. B. *J. Phys. Chem.* **1992**, *96*, 3591–3598.
(26) Toscano, J. P. *Adv. Photochem.* **2001**, *26*, 41–91.
(27) Toscano, J. P. In *Reviews of Reactive Intermediate Chemistry*; Platz, M. S., Moss, R. A., Jones, M., Jr., Eds.; John Wiley and Sons, Inc.: Hoboken, NJ, 2007; pp 183−206.
(28) Ma, C.; Kwok, W. M.; Chan, W. S.; Du, Y.; Kan, J. T. W.; Toy, P. H.; Phillips, D. L. *J. Am. Chem. Soc.* **2006**, *128*, 2558–2570.
(29) Besasson, B. V.; Gramain, J. C. *J. Chem. Soc., Faraday Trans. 1* **1980**, *76*, 1801–1810.
(30) Xu, M.; Wan, P. *Chem. Commun.* **2000**, 2147–2148.
(31) Ding, L.; Chen, X.; Fang, W. H. *Org. Lett.* **2009**, *11*, 1495–1498.
(32) Du, Y.; Xue, J.; Li, M.; Phillips, D. L. *J. Phys. Chem. A* **2009**, *113*, 3344–3352.
(33) Ramseier, M.; Senn, P.; Wirz, J. *J. Phys. Chem. A* **2003**, *107*, 3305–3315.
(34) He, Y.-Y.; Ramirez, D.-C.; Detweiler, C. D.; Mason, R. P.; Chignell, C. F. *Photochem. Photobiol.* **2003**, *77*, 585–591.
(35) Monti, S.; Manoli, F.; Sortino, S.; Morrone, R.; Nicolosi, G. P. *Phys. Chem. Chem. Phys.* **2005**, *7*, 4002–4008.
(36) Lhiaubet-Vallet, V.; Encinas, S.; Miranda, M. A. *J. Am. Chem. Soc.* **2005**, *127*, 12774–12775.
(37) Abad, S.; Bosca, F.; Domingo, L. R.; Gil, S.; Pischel, U.; Miranda, M. A. *J. Am. Chem. Soc.* **2007**, *129*, 7407–7420.

JP903234M